

Magnetic carbon – based nanocomposites for environmental applications: the case of arsenic and mercury removal from water[†]

Sara Gonçalves ¹, Tito Trindade ², Carlos Manuel Silva ² and Cláudia Batista Lopes ^{2,*}

¹ Department of Chemistry, University of Aveiro, Campus de Santiago 3810-193 Aveiro

² Department of Chemistry and CICECO, University of Aveiro, Campus de Santiago 3810-193 Aveiro; tito@ua.pt (T.T.); carlos.manuel@ua.pt (C.M.S.)

* Correspondence: claudia.b.lopes@ua.pt

† Presented at 4th International Online Conference on Nanomaterials, 5–9 May 2023; Available online: <https://iocn2023.sciforum.net/>.

Abstract: Arsenic and mercury are two elements that cause great concern in aquatic systems due to their toxic effects to the living organisms, bioaccumulation with time and biomagnification along the food chain. For these reasons continuous attempts to develop efficient water treatment methodologies have been made. Here, we report the synthesis and characterization of magnetic carbon-based nanostructures to remove As and Hg from aqueous solutions, and their concentration in a solid phase, promoting their recycling. The nanocomposites combine the magnetic properties of cobalt and manganese spinel ferrites properties with the ones of graphite nanoplatelets, exhibiting good sorption properties. In model solutions the removal efficiencies reach values of 80% using only a few milligrams per liter of nanocomposite.

Keywords: water remediation; toxic elements; graphite nanoplatelets; spinel ferrites

1. Introduction

Water is an essential resource to all human activities and to life in general, which is distributed inequitably around the world, with some populations living under water scarcity – a situation that is becoming more usually due to the impact of climate change [1]. Additionally, industrialization, population grow, and their needs have also contributed to the degradation and scarcity of safe water. Consequently, water issue it was made central to all components of the EU Green Deal and to several United Nation Sustainable Development Goals, starting with SDG6 on «clean water and sanitation». The mitigation of disastrous consequences of safe water scarcity is a worldwide challenge, and the scientific community should assume the responsibility for providing solutions based on scientific knowledge [1].

Arsenic and mercury are two elements that cause great concern in the aquatic systems. The chronic exposure of individuals to As could cause several injuries like cancer, and cardiovascular diseases, and even chromosome aberrations. According to the World Health Organization, the guideline value for As in drinking water is 10 µg/l, but in different regions of the globe, As concentrations can reach values significantly higher than 50 µg/l [2]. Mercury is neurotoxic, volatile, persistent, and bioaccumulates in the organisms. Due to their toxicity it is important to continue the research to improve the existent pollution control technologies [3]–[7].

From the available water cleaning technologies, adsorption is one of the most attractive due to its efficiency, reasonable cost, and simple operation mode. This is important for developing countries and for this reason, the adsorption process is generally preferred

Citation: Gonçalves, S.; Trindade, T.; Silva, C.M.; Lopes, C.B. *Eng. Proc.* **2021**, *3*, x. <https://doi.org/10.3390/xxxxx>

Published: 5 March

Publisher's Note: MDPI stays neutral with regard to jurisdictional claims in published maps and institutional affiliations.



Copyright: © 2021 by the authors. Submitted for possible open access publication under the terms and conditions of the Creative Commons Attribution (CC BY) license (<https://creativecommons.org/licenses/by/4.0/>).

since it meets this need due to its easy handling and the wide variation in available natural and synthetic sorbents. Additionally, because metal ions cannot be degraded by bioprocess and chemical reactions, currently adsorption is considered as the most effective way to remove metals and other inorganic elements from water [8].

Activated carbon was considered as one of the most successful adsorbents for many years due to its high adsorption capacity and thermal stability. Recently, graphene has been emerging as a promising sorbent for water treatment. However, for water applications, the graphene sheets exhibit problems such as poor solubility and tendency for agglomeration [9]. To overcome these limitations, researchers developed a few techniques to synthesize compounds, like graphene oxide and graphite-like nanoplatelets (GNP), which are structurally similar and can be produced by top-down methods from several carbon sources [10].

To facilitate the recovery of the sorbent after the treatment process we explored the preparation of magnetic nanocomposites. Magnetic field separation is more economical, selective, and rapid than filtration and centrifugation processes. The goal of this study was to synthesize nanocomposites that combine the sorption properties of GNPs with the magnetic properties of spinel ferrites of cobalt and manganese (CoFe_2O_4 ; MnFe_2O_4), conferring them the possibility of recovery from water when exposed to an external magnetic field. In line with the SDG6, we investigated the efficiency of these nanocomposites for adsorption of As and Hg from model solutions.

2. Materials and Methods

2.1. Chemicals

For the synthesis of the carbon-based composites the following chemicals were used without further purification: graphite flakes (EDM 99.95%, Graphit Kropfmühl), dimethylformamide (DMF, Carlo Erba), potassium hydroxide (KOH, Aldrich), potassium nitrate (KNO_3 , Aldrich), iron sulfate ($\text{FeSO}_4 \cdot 7\text{H}_2\text{O}$, AnalaR NORMAPUR VWR chemicals), manganese sulfate ($\text{MnSO}_4 \cdot \text{H}_2\text{O}$, Merck), cobalt chloride ($\text{CoCl}_2 \cdot 6\text{H}_2\text{O}$, Merck), nitric acid (HNO_3 , 63%, Merck), and ethanol ($\text{C}_2\text{H}_5\text{OH}$, PA, Carlo Erba).

For the batch experiments, certified commercial standards solutions of Hg ($\text{Hg}(\text{NO}_3)_2$, Merck) and As (H_3AsO_4 , Merck) with a concentration of 1000 ± 1 mg/l, and ultra-pure water (UPW) produced by a Millipore Integral 10 system, were used for the solutions preparation. Solutions of sodium hydroxide (NaOH) and nitric acid (HNO_3) were used for pH adjustments.

A Hg standard solution of 10 mg/l was prepared weekly in UPW by dilution from the certified standard solution of 1000 mg/l $\text{Hg}(\text{NO}_3)_2$. A second Hg standard solution of 100 $\mu\text{g/l}$ in UPW was prepared daily from the first one, and it was used for preparing the calibration standards for the Hg quantification. A As standard solution of 10 mg/l was prepared weekly in UPW by dilution from a certified standard solution of 1000 mg/l H_3AsO_4 , and it was used for the preparation of the calibration standards for As quantification.

2.2. Magnetic carbon-based nanocomposites synthesis

To obtain GNPs, graphite powder (5 g) was sonicated graphite (Sonics Vibra Cell Sonicator, VC70, 130 W, 20 kHz) in DMF (100 ml) for 5 h, in an ice bath replaced every 30 min. The presence of DMF facilitates the exfoliation of graphite by reducing the strength of the Van der Waals interactions between the adjacent layers of graphite. The GNPs were separated by centrifugation (1200 rpm, 20 min, Hettich, model rototfix), and the supernatant was transferred to a beaker, filtered, and washed repeatedly with water, and then ethanol. After, the solid was kept in a drying oven (Binder, model FD 23) at 40 °C until complete drying.

The MFe₂O₄/GNPs (M=Co or Mn) were prepared by in situ methodology preparing the spinel ferrites by oxidative hydrolysis in the presence of the GNPs. Briefly, deoxygenated water was added to 1.90 g of KOH and 1.52 g of KNO₃. This mixture was then heated at 60 °C (oil bath) under N₂ atmosphere and mechanically stirred (500 rpm, overhead stirrer, IKA). After the dissolution of the salts, GNPs (200 mg) were added to 25 ml of an aqueous solution containing 3.06 g of FeSO₄·7H₂O and 1.02 g of MnSO₄·H₂O. The resulting mixture was added dropwise to the alkaline solution and the stirring was increased to 700 rpm. This solution was left to react for 30 min. After, the mixture was left under N₂ at 90 °C for 4 h, without stirring. The resulting nanocomposite (MnFe₂O₄/GNPs) was collected by using a NdFeB magnet, and then repeatedly washed with water and ethanol, and dried in a drying oven (Binder, model FD 23) at 40 °C. For the synthesis of the CoFe₂O₄/GNPs, the 200 mg GNPs were added to 25 ml of UPW containing 3.06 g FeSO₄·7H₂O and 1.43 g of CoCl₂·6H₂O.

2.3. Magnetic carbon-based nanocomposites characterization

All the synthesized composites were characterized using transmission electron microscopy (TEM), X-ray diffraction (XRD), chemical analysis, Raman spectroscopy and magnetic characterization. To evaluate the morphological characteristics of the composites TEM analysis (Hitachi H-9000 TEM microscope) was performed. The structural characteristics of the composites were determined using X-ray diffraction. It was made sure the samples were completely dried, and subsequently the XRD spectra were obtained using a Philips X'Pert X-ray diffractometer equipped with a Cu K α monochromatic radiation source, in the range $2\theta = 3.5\text{--}70^\circ$. Raman spectra were obtained using a combined Raman confocal microscope (alpha 300 RAS+, WITec, Germany), equipped with Nd:YAG laser operating at 532 nm. The laser power used was 1mW. Magnetic measurements were performed using a Quantum Design MPMS3 SQUID-VSM. The Fe, Mn and Co composition was determined by microwave assisted acid digestion.

2.4. Removal of As and Hg from water

The capability of the MFe₂O₄/GNPs (M=Co or Mn) nanocomposites to remove Hg(II) and As(III) from model solutions was studied for mono element systems and different pH values. The removal capability of each material was assessed by exposing equal amounts of material (40 mg/l) to solutions of Hg(II) or As(III), containing initially 50 $\mu\text{g/l}$ and 1000 $\mu\text{g/l}$, of the respective element. Batch experiments were carried out for 24 h in 100 ml-Schott© glass flasks at 22 °C, with stirring (250 rpm), after dispersion of the sorbent in an ultra-sound bath. At 0 and 24 h, 25 ml of water aliquots were collected, preserved with NO₃ (pH <2) and stored at 4 °C until quantification. The liquid-solid separation was done by using a NdFeB magnet.

The pH effect on the removal capability of the nanocomposites was also studied, covering the whole range of groundwater pH values (4 to 9), under the previous operational conditions. At 0 and 24 h, 25 ml of water aliquots were collected, preserved, and stored as previously described. The results, from materials comparison and pH effect were expressed in terms of removal efficiency (R_A):

$$R_A = (C_{A0} - C_A / C_{A0}) \times 100 \quad (1)$$

where C_{A0} and C_A (both $\mu\text{g/l}$) are, respectively, the initial and at time t concentration of each element (A) in solution.

The experiments were done in duplicate, and controls (UPW spiked with Hg(II) or As(III) in the absence of composite) were running in parallel with the experiments, under the same operational conditions. Solution pH was adjusted with 0.1 mol/l NaOH or 0.1 mol/l HNO₃ solutions. Mercury quantification was performed by cold vapor atomic fluorescence spectroscopy on a flow-injection cold vapor atomic fluorescence spectrometer (hydride/vapor generator PS Analytical Model 10.003, coupled to a PS Analytical Model 10.023 Merlin atomic fluorescence spectrometer), using SnCl₂ solution as reducing agent

(10% m/v). The limit of quantification was 0.1 $\mu\text{g/l}$ Hg and the precision and accuracy <10%. Calibration curve (0.1 – 0.5 $\mu\text{g/l}$) was obtained using five standards prepared by diluting an appropriate volume of Hg standard solution (100 $\mu\text{g/l}$) in 2% HNO_3 . Arsenic quantification was performed by hydride generation atomic fluorescence spectroscopy (PS Analytical Model 10.033 Excalibur atomic fluorescence spectrometer), using a NaBH_4 solution as reducing agent. The limit of quantification was 10 $\mu\text{g/l}$ As and the precision and accuracy <10%. The samples were diluted 2 - 20 times, depending on the expected As concentrations, in 50 ml flasks with a 25% v/v HCl and 50% m/v KI with 10% m/v ascorbic acid solution (blank reagent). Calibration curve (10 – 80 $\mu\text{g/l}$) was obtained using five standards prepared by diluting the As standard solution (10 mg/l) in the blank reagent. All glassware used in the sorption essays was immerse in acid solution (HNO_3 25% v/v) for at least 12 h, then rinsed with UPW, before use.

3. Results and Discussion

3.1. Magnetic carbon-based nanocomposites characterization

3.1.1. TEM

The TEM images of the nanocomposites show the presence of CoFe_2O_4 and MnFe_2O_4 nanoparticles, with a spherical shape and an average size below 100 nm, attached to a lighter shaded substrate (GNPs) (Figure 1). The images also show different exfoliate degree of the graphite, with darker and lighter areas.

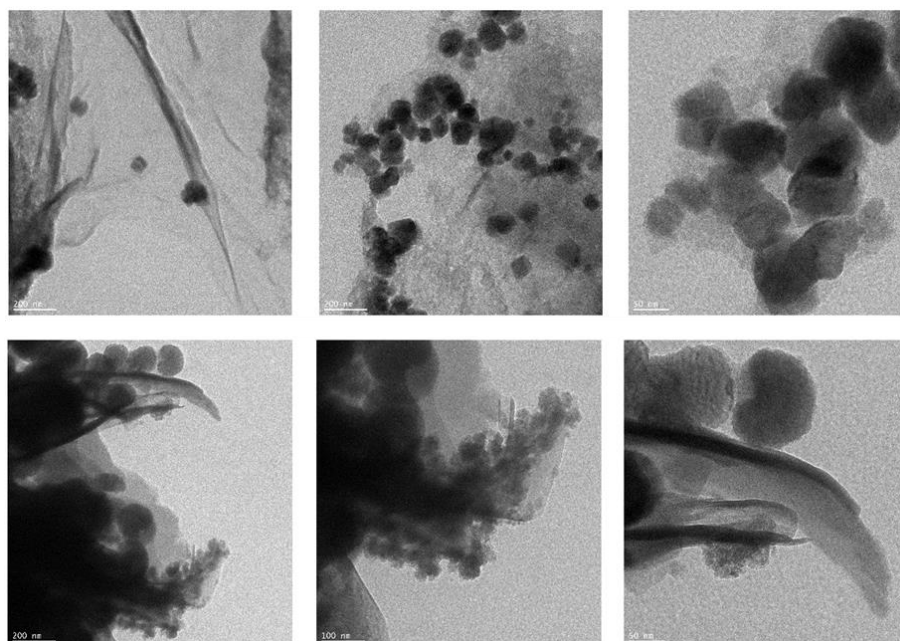


Figure 1. TEM images of $\text{CoFe}_2\text{O}_4/\text{GNPs}$ (top) and $\text{MnFe}_2\text{O}_4/\text{GNPs}$ (down).

The diffractograms of the nanocomposites (not shown) confirm the presence of cobalt- and manganese ferrites and GNPs. They display an intense peak at $2\theta=26.56^\circ$ that corresponds to the interlayer (002) planes distance d 0.34 nm in the graphitic structure. The remaining XRD peaks are indexed from the JCPDS cards for CoFe_2O_4 (No. 22-1086) and MnFe_2O_4 (No. 73-1964). The reflections at $2\theta = 18.2^\circ$ (111), 29.9° (220), 35.2° (311), 42.8° (400), 56.6° (511), 62.1° (440) (and the weak reflections at $2\theta = 53.2^\circ$ (422) and 89.0° (731)) confirmed the presence of MnFe_2O_4 in the $\text{MnFe}_2\text{O}_4/\text{GNPs}$. The $\text{CoFe}_2\text{O}_4/\text{GNPs}$ XRD spectrum showed weaker reflections than the one of manganese ferrite. Although generally weak, the reflections at $2\theta = 18.3^\circ$ (111), 35.5° (311), 43.2° (400), 57.1° (511), 62.1° (440) (and the very weak 30.6° (220) and 88.5° (731)) confirmed the presence of CoFe_2O_4 .

The major bands in the Raman spectrum of the cobalt-ferrite nanocomposite reflected a typical spinel structure. The band at $\sim 316\text{ cm}^{-1}$ was attributed to the E-site mode and bands at $\sim 616\text{ cm}^{-1}$ and $\sim 687\text{ cm}^{-1}$ were attributed to the A-site modes of CoFe_2O_4 , in accordance with literature. Additional bands at $\sim 474\text{ cm}^{-1}$, $\sim 190\text{ cm}^{-1}$ and $\sim 290\text{ cm}^{-1}$ were attributed to the O-site mode, which reflects the local lattice effect in the octahedral sublattice. Also, for the manganese-ferrites, the spinel structure was reflected in the Raman spectrum. The band at $\sim 333\text{ cm}^{-1}$ was attributed to the E-site mode and the band at $\sim 627\text{ cm}^{-1}$ was attributed to A-site modes of MnFe_2O_4 , in accordance with literature. Both nanocomposites show the D mode and the G and 2D peaks represented by the bands at $\sim 1353\text{ cm}^{-1}$, $\sim 1580\text{ cm}^{-1}$ and $\sim 2705\text{ cm}^{-1}$ characteristic of graphite.

The chemical composition of the nanocomposites is displayed in Table 1. The ratios of Fe/Co and Fe/Mn agree with the expected values.

Table 1. Co, Fe and Mn concentrations of the materials, determined via acid digestion.

Nanocomposite	[Fe] (mg/l)	[Co] (mg/l)	[Mn] (mg/l)	Fe/Co	Fe/Mn
$\text{CoFe}_2\text{O}_4/\text{GNPs}$	79.8	43.0	-	1.9	-
$\text{MnFe}_2\text{O}_4/\text{GNPs}$	80.9	-	40.2	-	2.0

From the magnetic measurements it was observed that both materials quickly approach towards saturation when exposure to an external magnetic field. The values obtained for the saturation magnetization at room temperature (30 emu/g), combined with the visual observations, evidence the necessary magnetic properties of both materials. More, the saturation magnetization values found are in the range of the reported values for similar sorbents and are appropriate for magnetically assisted removal.

3.2. Removal of As and Hg from water

In adsorption, the solution pH is one of the main parameters that may have a strong impact in the efficiency of the process. The removal efficiency obtained for each contaminant and nanomaterial, for different solution pH are shown in Figure 2.

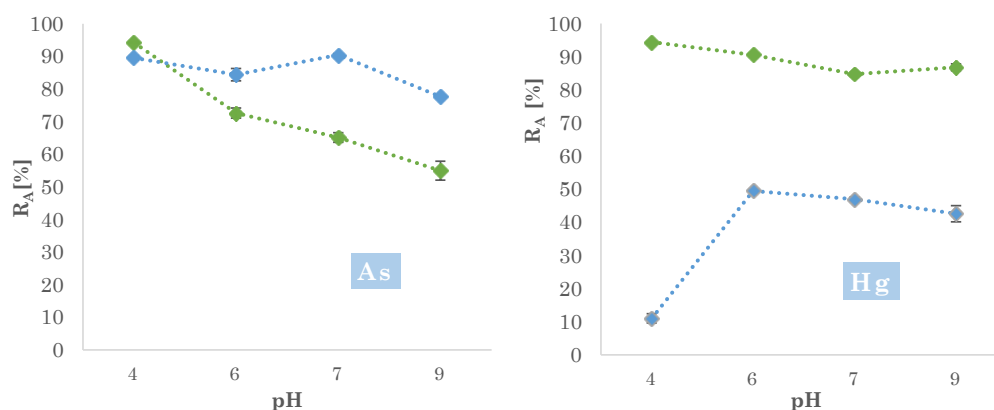


Figure 2. Removal efficiency of magnetic carbon-based nanocomposites toward arsenic (As) and mercury (Hg) ($\text{MnFe}_2\text{O}_4/\text{GNPs}$ - green points; $\text{CoFe}_2\text{O}_4/\text{GNPs}$ - blue points).

It was found that $\text{MnFe}_2\text{O}_4/\text{GNPs}$ has a higher affinity for Hg than $\text{CoFe}_2\text{O}_4/\text{GNPs}$ throughout the pH range studied, and similar efficiency to $\text{CoFe}_2\text{O}_4/\text{GNPs}$ for As at pH 4.

For pH values between 6 and 9 the As removal efficiency is higher for CoFe₂O₄/GNPs than for MnFe₂O₄/GNPs. Differences in the removal efficiency between nanocomposites and toward contaminants may be related to the different speciation of As and Hg ions in solution according to pH and to the surface charge of the materials.

4. Conclusions

Magnetic carbon-based nanocomposites were successfully synthesized by attaching spinel ferrites (MnFe₂O₄ and CoFe₂O₄) to graphite nanoplatelets and evidence good sorption efficiency toward As and Hg water contaminants.

Author Contributions: “Conceptualization, Cláudia B. Lopes; methodology, Sara Gonçalves; resources, Tito Trindade; writing—original draft preparation, Sara Gonçalves; writing—review and editing, Cláudia B. Lopes; supervision, Carlos M. Silva and Cláudia B. Lopes.; funding acquisition, Cláudia B. Lopes. All authors have read and agreed to the published version of the manuscript.

Funding: FCT – Foundation for Science and Technology provided financial support to C.B. Lopes (2021.03739.CEECIND). This work was developed within the scope of the project GraphChem (2022.04409.PTDC) and CICECO-Aveiro Institute of Materials, UIDB/50011/2020, UIDP/50011/2020 & LA/P/0006/2020, financed by national funds through the FCT/MEC (PIDDAC).

References

- [1] A. C. Estrada *et al.*, “Colloidal nanomaterials for water quality improvement and monitoring,” *Front Chem*, vol. 10, Sep. 2022, doi: 10.3389/FCHEM.2022.1011186.
- [2] P. L. Smedley and D. G. Kinniburgh, “A review of the source, behaviour and distribution of arsenic in natural waters,” *Applied Geochemistry*, vol. 17, no. 5, pp. 517–568, May 2002, doi: 10.1016/S0883-2927(02)00018-5.
- [3] P. C. Pinheiro *et al.*, “Ferromagnetic sorbents based on nickel nanowires for efficient uptake of mercury from water,” *ACS Appl Mater Interfaces*, vol. 6, no. 11, pp. 8274–8280, Jun. 2014, doi: 10.1021/AM5010865.
- [4] M. Abid *et al.*, “Arsenic(V) biosorption by charred orange peel in aqueous environments,” *Int J Phytoremediation*, vol. 18, no. 5, pp. 442–449, May 2016, doi: 10.1080/15226514.2015.1109604.
- [5] P. Figueira, M. A. O. Lourenço, E. Pereira, J. R. B. Gomes, P. Ferreira, and C. B. Lopes, “Periodic mesoporous organosilica with low thiol density - A safer material to trap Hg(II) from water,” *J Environ Chem Eng*, vol. 5, no. 5, pp. 5043–5053, Oct. 2017, doi: 10.1016/J.JECE.2017.09.032.
- [6] D. S. Tavares, C. B. Lopes, J. C. Almeida, C. Vale, E. Pereira, and T. Trindade, “Spinel-type ferrite nanoparticles for removal of arsenic(V) from water,” *Environmental Science and Pollution Research*, vol. 27, no. 18, pp. 22523–22534, Jun. 2020, doi: 10.1007/S11356-020-08673-9.
- [7] S. P. Cardoso, T. L. Faria, E. Pereira, I. Portugal, C. B. Lopes, and C. M. Silva, “Mercury removal from aqueous solution using ETS-4 in the presence of cations of distinct sizes,” *Materials*, vol. 14, no. 1, pp. 1–13, Jan. 2021, doi: 10.3390/MA14010011.
- [8] M. Z. A. Zaimee, M. S. Sarjadi, and M. L. Rahman, “Heavy Metals Removal from Water by Efficient Adsorbents,” *Water 2021, Vol. 13, Page 2659*, vol. 13, no. 19, p. 2659, Sep. 2021, doi: 10.3390/W13192659.
- [9] A. Joseph, V. Sajith, and C. Sarathchandran, “Graphene: The magic material,” *Handbook of Carbon-Based Nanomaterials*, pp. 517–549, Jan. 2021, doi: 10.1016/B978-0-12-821996-6.00001-4.
- [10] N. Rao, R. Singh, and L. Bashambu, “Carbon-based nanomaterials: Synthesis and prospective applications,” *Material Today Proc*, vol. 44, pp. 608–614, Jan. 2021, doi: 10.1016/J.MATPR.2020.10.593.